Available online at www.sciencedirect.com
SCIENCE DIRECT
Polymer 46 (2005) 5299–5307
polymer
www.elsevier.com/locate/polymer

Very stable, highly electroactive polymers of zinc(II)-5,15-bisthienylphenyl porphyrin exhibiting charge-trapping effects

Guangtao Li[a,*], Sheshanath Bhosale[b], Shengyang Tao[a], Ruirong Guo[a], Sidhanath Bhosale[b], Fengting Li[a], Yihe Zhang[c], Tianyu Wang[b], Jürgen-Hinrich Fuhrhop[b,**]

[a]*Key Lab of Organic Optoelectronics and Molecular Engineering, Department of Chemistry, Tsinghua University, 100084 Beijing, China*
[b]*Freie Universität Berlin, Institut für Organische Chemie, Takustr. 3, 14195 Berlin, Germany*
[c]*Technical Institute of Physics and Chemistry, Chinese Academy of Sciences, Beijing 100080, China*

Received 14 December 2004; received in revised form 18 March 2005; accepted 14 April 2005

Abstract

Two new thiophene-substituted porphyrins and their zinc complexes were synthesized and electropolymerized via thiophene units on different electrode surfaces. Electrochemical characterizations show that the resultant polythiophenemetalloporphyrin hybrid materials are highly electroactive and exhibit remarkable higher electrochemical stability. Interestingly, they exhibit a charge-trapping effect. A mechanism for the observed charge-trapping phenomenon was proposed and supported by using model compounds. The deposited polymer films on different electrode surfaces exhibit a homogeneous morphology and possess good processability (soluble in polar solvents such as DMSO or DMF). Besides electrochemical method, UV/vis, NMR, FTIR, TEM and SEM were employed to characterize the new hybrid material.

Keywords: Electropolymerization; Electroactive polymer; Porphyrin

1. Introduction

Porphyrins and their metal complexes are found in many natural systems, where they play an essential role as photoactive, redox, guest-binding, and catalytic entities. These properties make them ideal candidate for developing electrocatalysis, chemical and biological sensors or for solar energy conversion on electrode surfaces [1–5].

Among various immobilization methods such as chemisorption [6,7], condensation reactions of porphyrin side chains with functionalized electrodes [8,9], self-assembly [10–13] as well as the uptake of charged porphyrins by ion-exchange polymer coatings [14], electrochemical polymerization of a suitably designed monomer provides a facile approach for attaching porphyrins to electrode surface. In general, this method allows production of homogeneous, adherent electroactive porphyrin films at the expected potential, and the amount of deposited materials can be easily controlled by the number of potential sweep or the total charge passed during polymerization process [3]. The oxidative electropolymerization of metalloprotoporphyrin IX complex via the vinyl substituents at the porphyrin periphery, and porphyrins with polymerizable phenol, pyrrole or aniline substituents were extensively investigated [4,15–19]. Recently, thiophene mediated electropolymerization was also described [20–26]. The majority of the formed metalloporphyrin films, however, showed only a moderate electrochemical stability.

In this work, we report the synthesis of highly electroactive polythiophenemetalloporphyrin hybrid material that exhibits remarkable higher electrochemical stability. Furthermore, it exhibits a charge-trapping effect.

* Corresponding authors. Tel./fax: +86 10 62785967.
** Tel./fax: +49 30 83855394.
E-mail addresses: lgt@mail.tsinghua.edu.cn (G. Li), fuhrhop@chemie.fu-berlin.de (J.-H. Fuhrhop).

0032-3861/$ - see front matter © 2005 Elsevier Ltd. All rights reserved.
doi:10.1016/j.polymer.2005.04.029

2. Experimental section

2.1. Chemicals

Thiophene (Aldrich), tributyltin chloride (Fluka), 3,4-(ethylenedioxy)thiophene (Aldrich), 4-bromobenzaldehyde (Fluka), DDQ (Fluka), trifluoroacetic acid (Fluka), bis(triphenylphosphine)palladium dichloride (Fluka), and zinc tetraphenyporphyrin (Aldrich) were used as received. 5-Phenyldipyrromethane was prepared following the method reported by Lindsey [27]. 5,5′-Bistributylstannyl-2,2′-bi(3,4-ethylenedioxythiophene) was synthesized according to the procedure described by Cava [28]. All solvents used for synthesis were freshly distilled prior to use. For electrochemical measurements, the electrochemical grade solvents and electrolyte salts such as methylene chloride (Baker) and tetrabutylammonium hexafluorophosphate (Fluka) were used.

2.2. Synthesis

2.2.1. 4-(2-Thienyl)benzaldehyde

2.77 g (15 mmol) 4-bromobenzaldehyde and 0.53 g (0.75 mmol) $Cl_2Pd(PPh_3)_2$ were dissolved in 100 ml of DMF. To this mixture 8.4 g (22.5 mmol) tributylstannyl thiophene was added. Under nitrogen atmosphere the reaction mixture was heated at 80 °C for 14 h. The reaction mixture was cooled to room temperature, diluted with Et_2O, and washed with diluted NH_4Cl for several times. The organic layer was collected and filtered through a short silica pad. After the removal of solvent under reduced pressure a yellow solid was obtained. This solid was thoroughly washed with hexane, filtered and dried in vacuo to afford 1.7 g of yellow powder (60%). ^{1}H NMR ($CDCl_3$): $\delta = 9.98$ (s, 1H), 7.92 (d, 2H), 7.72 (d, 2H), 7.48 (d, 1H), 7.41 (d, 1H), 7.21 (m, 1H). MS (EI) $m/z = 188$ (M^+). Elem. Anal.: $C_{11}H_8OS$ (188.25) Calcd: C 70.18; H 4.28; S 17.03. Found: C 70.34; H 4.21; S 17.21.

2.2.2. 4-(2-(3,4-Ethylenedioxy)thienyl)benzaldehyde

This compound was synthesized from 2-tributylstannyl-3,4-ethylenedioxythiophene by the same method described above as yellow powder (53%) ^{1}H NMR ($CDCl_3$): $\delta = 9.89$ (s, 1H), 7.87 (d, 2H), 7.69 (d, 2H), 6.12 (s, 1H). 4.39 (t, 2H), 4.42 (t, 2H). MS (EI) $m/z = 246$ (M^+). Elem. Anal.: $C_{13}H_{10}O_3S$ (246.28) Calcd: C 63.40; H 4.09; S 13.02. Found: C 63.34; H 4.12; S 13.21.

2.2.3. 5,15-Bis(4-(2-thienyl)phenyl)-10,20-diphenylporphyrin

4-(2-Thienyl)benzaldehyde (1.13 g, 6 mmol) and 5-phenyldipyrromethane (1.33 g, 6 mmol) were dissolved in 1 l of dried CH_2Cl_2, and the solution was stirred magnetically at room temperature under a slow stream of nitrogen. After 60 min, 120 μl TFA was added and the reaction mixture was shielded from lighting. After 20 h, DDQ (4.43 g, 18 mmol) was given and the reaction was continued for further 2 h. The solution was then concentrated to about 50 ml by rotary evaporation, and the residue was purified by silica column chromatography using CH_2Cl_2/diethyl ether as eluent, affording the desired compound (yield 27%). ^{1}H NMR ($CDCl_3$): $\delta = 8.92$ (d, 4H), 8.86 (d, 4H), 8.16 (m, 8H), 8.04 (m, 4H), 7.78 (m, 6H), 7.58 (d, 2H), 7.50 (m, 2H), 7.42 (d, 2H), −2.84 (s, 2H); MS (FAB^+) $m/z = 778$ (M + 1).

2.2.4. 5,15-Bis(4-(2-(3,4-ethylenedioxy)thienyl)phenyl)-10,20-diphenylporphyrin

This compound was synthesized in a similar fashion described above with exception that instead of 4-(2-thienyl)benzaldehyde, 4-(2-(3,4-ethylenedioxy)thienyl)-benzaldehyde was used (yield 30%). ^{1}H NMR ($CDCl_3$): $\delta = 8.94$ (d, 4H), 8.87 (d, 4H), 8.20 (m, 8H), 8.08 (m, 4H). 7.81 (m, 6H), 6.46 (s, 2H), 4.43 (t, 4H), 4.34 (t, 4H), −2.83 (s, 2H); MS (FAB^+) $m/z = 895$ (M + 1).

2.2.5. 5,5′-Bisphenyl-2,2′-bi(3,4-ethylendioxythiophene)

5,5′-Bistributylstannyl-2,2′-bi(3,4-ethylenedioxythiophene) (5 g, 17.7 mmol), bromobenzene (5.5 g, 37.4 mmol) and $Pd(PPh_3)_2Cl_2$ (2 g, 1.7 mmol) were dissolved in 100 ml dried THF. The reaction mixture was refluxed under argon for 10 days. After cooled to room temperature, the mixture was concentrated to 10 ml. The precipitate was filtered and washed throughly with ethanol and ether, affording a brown solid (45%). ^{1}H NMR ($CDCl_3$): $\delta = 7.89$ (m, 4H), 7.74 (m, 6H), 4.46 (t, 8H); MS (EI) $m/z = 434$ (M). Elem. Anal.: $C_{24}H_{18}O_4S_2$ (343.53) Calcd: C 66.34; H 4.18; S 14.76. Found: C 66.44; H 4.12; S 14.81.

2.3. Electrochemistry

The determination of the oxidation potentials of the monomer **1** and **2** as well as their electropolymerization was carried out with a HEKA PG 28 potentiostat in a one-compartment three-electrode cell. The anode was a platinum disk electrode (16 mm^2) polished with 0.05 μm diamond paste and then sonicated in distilled water before use. The counter electrode was a Pt wire. An Ag/AgCl electrode was chosen as reference electrode. Before each electrochemical experiment the reaction medium was purged with argon for 10 min at room temperature. For UV/vis and SEM measurements, ITO glass was used as working electrode.

2.4. Characterization

^{1}H spectroscopic data were obtained with a Bruker AM 270 SY in $CDCl_3$ or CD_3SOCD_3 as solvent using TMS as standard. IR spectra were recorded on a Perkin Elmer 580B with data station PE 360 (KBr). MS data were obtained by means of a Finnigan MAT 112b and a Finnigan MAT 711. Elementary analyses were performed with a Perkin Elmer

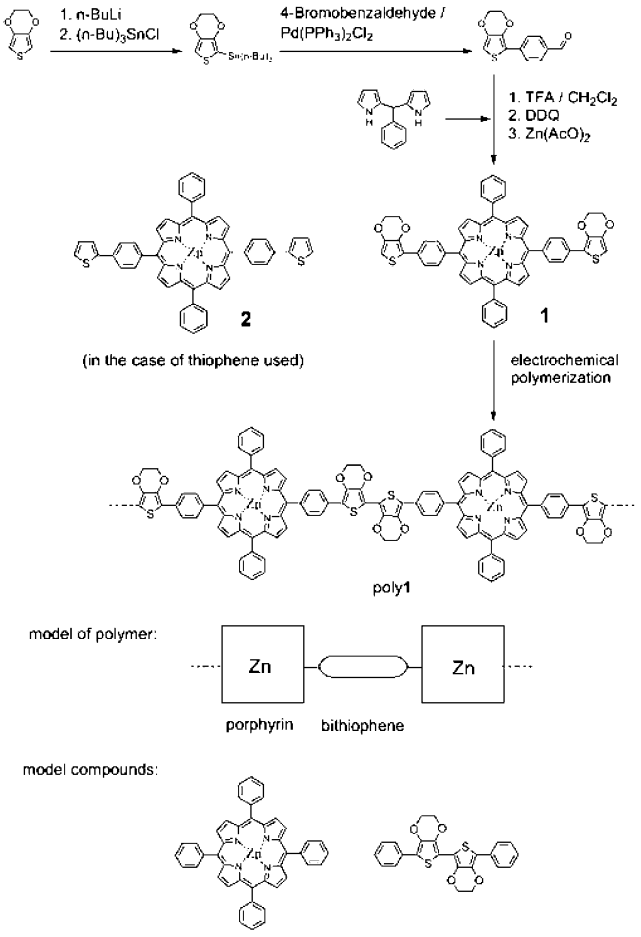

Scheme 1. Synthesis of thiophene-substituted porphyrins and the model of the obtained polymer chains.

2400 CHNS analyzer. The reflectance FTIR spectra were recorded by means of a Nicolet 800-FTIR spectrometer. SEM was performed on a Hitachi S-4500FE operating at 2 kV. The formed polymer conducted sufficiently and therefore did not require any coating prior to imaging.

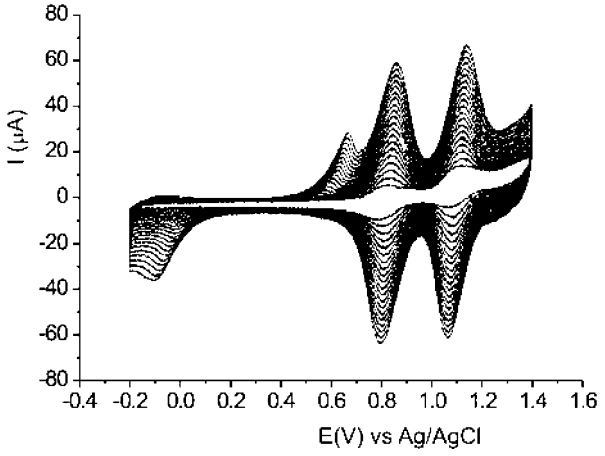

Fig. 1. Oxidative electropolymerization of monomer **1** on a Pt electrode surface by repeated potential scans at 100 mV/s between −0.2 and +1.4 V vs. Ag/AgCl in 0.1 M $TBAPF_6/CH_2Cl_2$ containing 0.1 mM monomer **1**.

TEM samples were prepared by dropping 10 μl aliquots of DMSO solution of polymer onto a holey carbon coated copper grid. After deposition for 1 min, the remaining solution was blotted with a filter paper and the remaining polymers were stained by using 1% phosphotungstate. The polymer fibres were imaged using a Philips M12 transmission electron microscope operated at 100 kV.

3. Results and discussion

New monomers were designed to favor the formation of porphyrin macrocycles with electrochemically polymerizable thiophene moieties on alternating subunits (Scheme 1). This arrangement should allow formation of linear polymer chains with the metal center in direct electronic communication with the conjugated polymer backbone. The thiophene-substituted benzaldehyde was produced by a palladium catalyzed Stille-coupling. Condensation of the resulting aldehyde with 5-phenyldipyrromethane using TFA in CH_2Cl_2 followed by oxidation with DDQ [27,29] gave the desired porphyrin **1** and **2** in 20–30% yields. Metallation with zinc acetate afforded the zinc complex in 50–70% yields. Thiophene and 3,4-ethylenedioxythiophene were chosen as polymerizable moieties in these porphyrin monomers, respectively (Scheme 1).

Polymeric films of monomer **1** can be readily deposited on Pt, GC, ITO or Au electrodes by repetitive potential scanning between −0.2 and +1.4 V (vs. Ag/AgCl). Methylene chloride, acetonitrile or nitrobenzene have been used as solvents for these polymerization processes. Representatively, Fig. 1 shows the evolution of the cyclic voltammograms on Pt electrode from a 0.1 mM monomer **1** solution in 0.1 M $TBAPF_6/CH_2Cl_2$ over the potential range from −0.2 to +1.4 V. The resulting polymer film remained electroactive during polymerization process so that the oxidative and reductive current peaks continuously increased with each successive potential cycle. This is characteristic for nonpassivating electropolymerization. The polymer growth remained steadily over a period of 1 h. As a result, a thick and self-supporting film was obtained. These results indicate that the polymer formed possesses enough electrical conductivity to maintain the polymer growth process. Thin deposited films are strongly adherent to different electrode surfaces. Upon the increase of the film thickness, the adherence of the deposited polymer films to electrode surfaces becomes poor. In the case of monomer **2**, however, no polymer was formed due to low solvation by applied solvents.

After 20 scanning cycles (Fig. 1) the Pt electrode was coated by a dark brown and adherent thin polymer film (**poly1**). After thoroughly rinsing, it was transferred to a CH_2Cl_2 + 0.1 M $TBAPF_6$ solution free of monomers. The cyclic voltammogram of this modified electrode exhibited the regular electrochemical response of the immobilized zinc porphyrin characterized by two reversible one-electron

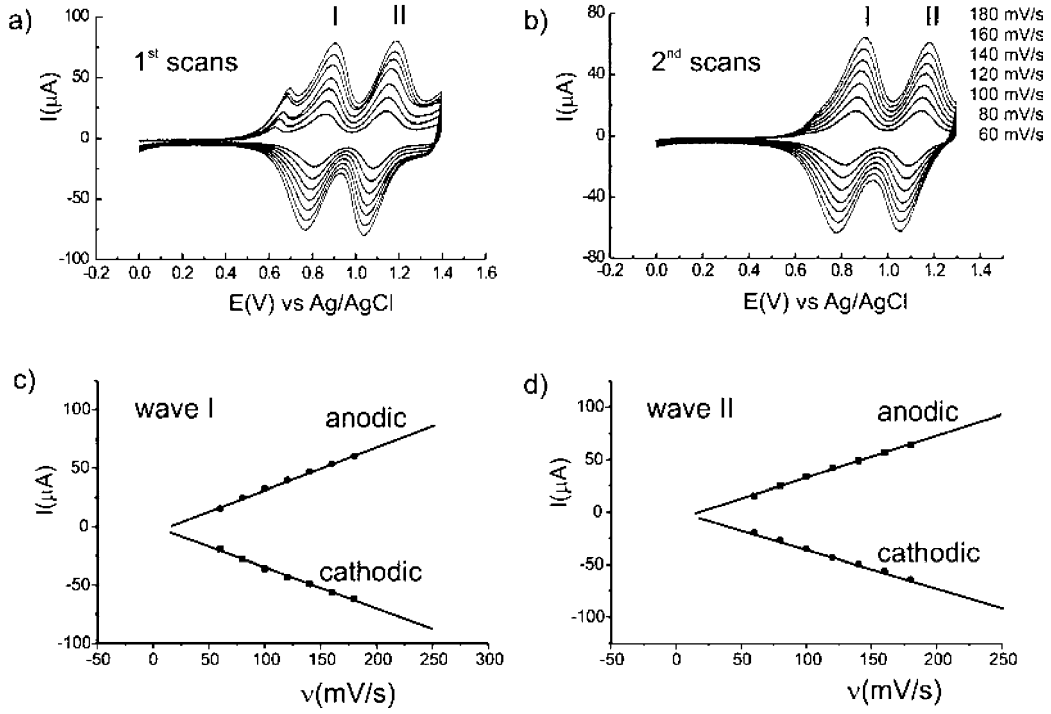

Fig. 2. Cyclic voltammetry as a function of sweep rate for a Pt/**poly1** electrode: (a) the first scans, (b) the second scans, and peak currents for wave I and II as a function of the scan rate, (c) wave I, (d) wave II.

porphyrin ring oxidations at $E_{1/2}=0.84$ V [ZnP]/[ZnP]$^{+\cdot}$ and $E_{1/2}=1.06$ V [ZnP]$^{+\cdot}$/[ZnP]$^{2+}$ (Fig. 2(a) and (b)) [30]. The ratios of I_{pa} (anodic peak current) to I_{pc} (cathodic peak current) in both surface waves remained equal to one at different potential sweeping rates. The potential difference between oxidation and reduction peaks (ΔE_p) was between 50 and 100 mV, depending on potential scan rate (60–180 mV/s, Fig. 2(a) and (b)). These parameters clearly revealed that the formed porphyrin film is highly electroactive [2]. The linear increase of peak current with potential scan rates indicates surface-confined redox species, and is not controlled by diffusion rates (Fig. 2(c) and (d)). The fact that even at faster potential scan rates the linear relationship is kept, indicates that the synthesized **poly1** possesses higher electron self-exchange rate. Integrating the charge under these redox waves gave 5×10^{-8} mol/cm^2 coverage of electroactive sites on electrode surface. The coverage of the deposited polymer can be readily and reproducibly adjusted by varying the number of cyclical potential scans. Depending on the preparation condition, electroactive polymer layers ranging from 5×10^{-10} to 5×10^{-6} mol/cm^2 have been deposited on the electrode surfaces. This corresponds to several to several thousands porphyrin monolayers, assuming that porphyrin lies flat on electrode surface and each layer has a thickness of 0.6 nm.

Comparing the surface waves in Fig. 2, it is clearly seen that a sharp prepeak always arises at the foot of the first oxidation wave (Fig. 2(a)) and disappears in the second scan (Fig. 2(b)). The magnitude of this prewave increases and the peak potential shifts with scan rates, moving closer to the main waves at the faster sweep rates. If the potential scan range was restricted to the positive range, the prepeak completely vanished after the first scan and the resulting state remained stable in following scans (Fig. 4). Only when the potential was switched to -0.2 V and remained at this potential for 2 min, the disappeared prepeak is fully restored after a sweep in the positive range up to the oxidation of the porphyrin macrocycles. This process is perfectly reversible and reproducible. This observed feature is not dependent on the nature of solvent, supporting electrolyte or the electrode substrate. The same prewaves are seen in CH_3CN/$TBAClO_4$, CH_2Cl_2/$TBAClO_4$, CH_2Cl_2/$TBAPF_6$ and on Pt, ITO, GC or Au electrodes. These results indicate that the observed behavior is not the result of impurities, but involves a charge-trapping phenomenon or current rectification.

Murray group is first to report the rectification phenomenon on electrodes using bilayer structure [31,32]. They deposited two physically discrete layers of electroactive materials of different redox potentials on a conductor electrode. When the redox potentials were chosen appropriately, the electron transfer between the outer electroactive layer and the underlying electrode is forced to occur catalytically by electron-transfer mediation through redox states of the inner electroactive layer. Wrighton et al. found that such feature is also realizable, when two different redox units were incorporated in a polymer chain and the structure of the polymer prevented one of both redox subunits from direct charge transport to and from the electrode [33–36]. Considering all results described in literatures, we believe that the finding by Wrighton should be responsible for our

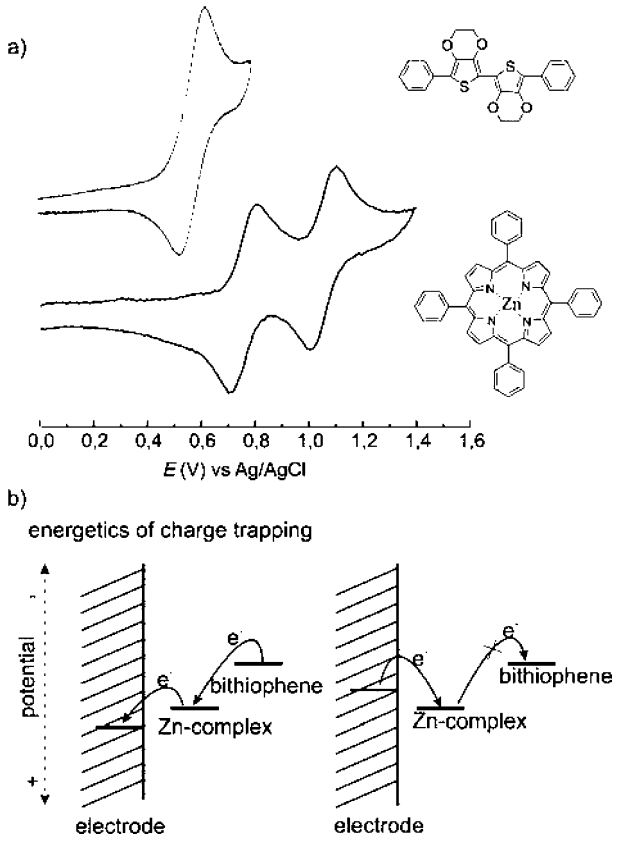

Fig. 3. (a) Cyclic voltammetry of a Pt electrode in 0.1 M $TBAPF_6/CH_2Cl_2$ containing 0.1 mM 5,5′-bisphenyl-2,2′-bi(3,4-ethylenedioxythiophene) or Zn complex of tetraphenylporphyrin. $\nu = 100$ mV/s. (b) schematic representation of electron energy level for a Pt/**poly1** electrode.

case. In fact, due to the well-known minimal π-overlap between the aryl ring and porphyrin macrocycle [1], the synthesized polymer (**poly1**) can be considered to consist of two isolated redox systems: porphyrin and 5,5′-bisphenyl-2,2′-bithiophene (Scheme 1). The blocky porphyrin may cause a spatial segregation and prevent bithiophene units from direct contacting with electrode surface, and therefore undergoing effective electron-exchange with electrode surface [32].

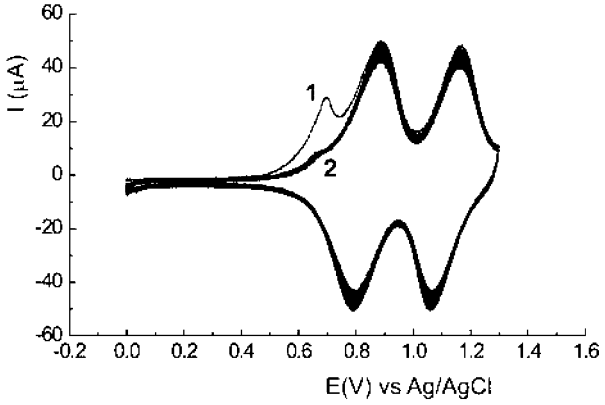

Fig. 4. Repeated cyclic voltammograms of a Pt electrode coated with **poly1** in 0.1 M $TBAPF_6/CH_2Cl_2$ solution, $\nu = 100$ mV/s. (1) first cycle, (2) 2–1000 cycles.

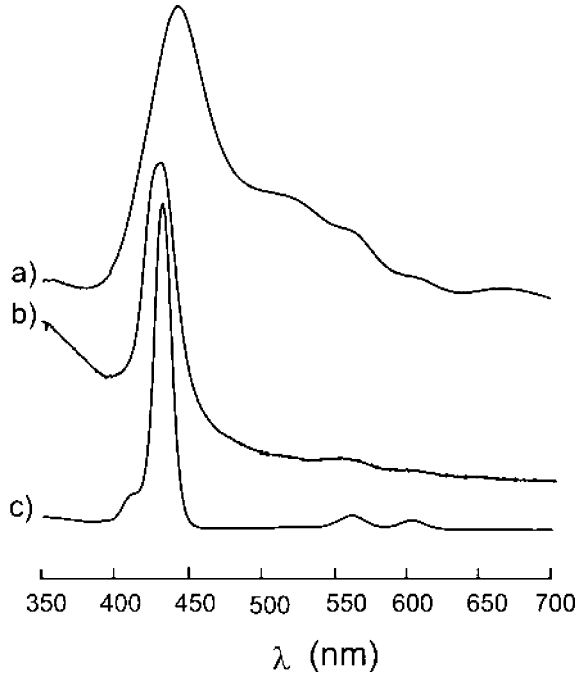

Fig. 5. UV/vis spectra of **poly1** film on transparent ITO electrode (a), dissolved **poly1** in DMSO (b) as well as 0.1 μM monomer **1** in DMSO (c).

Electrochemical characterization of synthesized model compounds: 5,5′-bisphenyl-2,2′-bi(3,4-ethylendioxythiophene) and zinc complex of tetraphenylporphyrin in solution confirmed our assumption (Scheme 1 and Fig. 3(a)). Zinc porphyrin displays the two one-electron oxidation of porphyrin ring at the same potentials: 0.78 and 1.06 V (vs. Ag/AgCl). The oxidation of 5,5′-bisphenyl-2,2′-bi(3,4-ethylenedioxythiophene), however, occurs at 0.61 V, which is much lower than peak potential of prepeak (∼0.7 V). It is obvious that, due to the electronic separation described above, the 5,5′-bisphenyl-2,2′-bi(3,4-ethylene-dioxy-thiophene) subunit in **poly1** will be electroactive only after the oxidation of porphyrin ring has taken place. As a result, the oxidized state of bithiophene is trapped when the potential scan is reversed. The scheme in Fig. 3 presents the energy level diagram of our polymer system.

The electrochemical stability of **poly1** coated electrode was investigated by scanning the electrode potential one thousand times over the oxidation wave (Fig. 4). Only 5% decrease in the intensity of the peak currents occurred (Fig. 4). Especially, the previously reported instability of zinc complex of the polyporphyrinate dication [37] was not observed in **poly1**. Compared to the reported porphyrin polymers including the polymers from electropolymerization of porphyrin with pyrrole [4,16–18,37,38], the new porphyrin polymer exhibits remarkable higher electrochemical stability. The bases of this property are presumably the better thermal, electrochemical stability as well as the highly electrical conductivity of poly(ethylenedioxythiophene) as compared to polyaniline and polythiophene [23,39–41].

The UV/vis absorption spectrum of the monomer **1** in

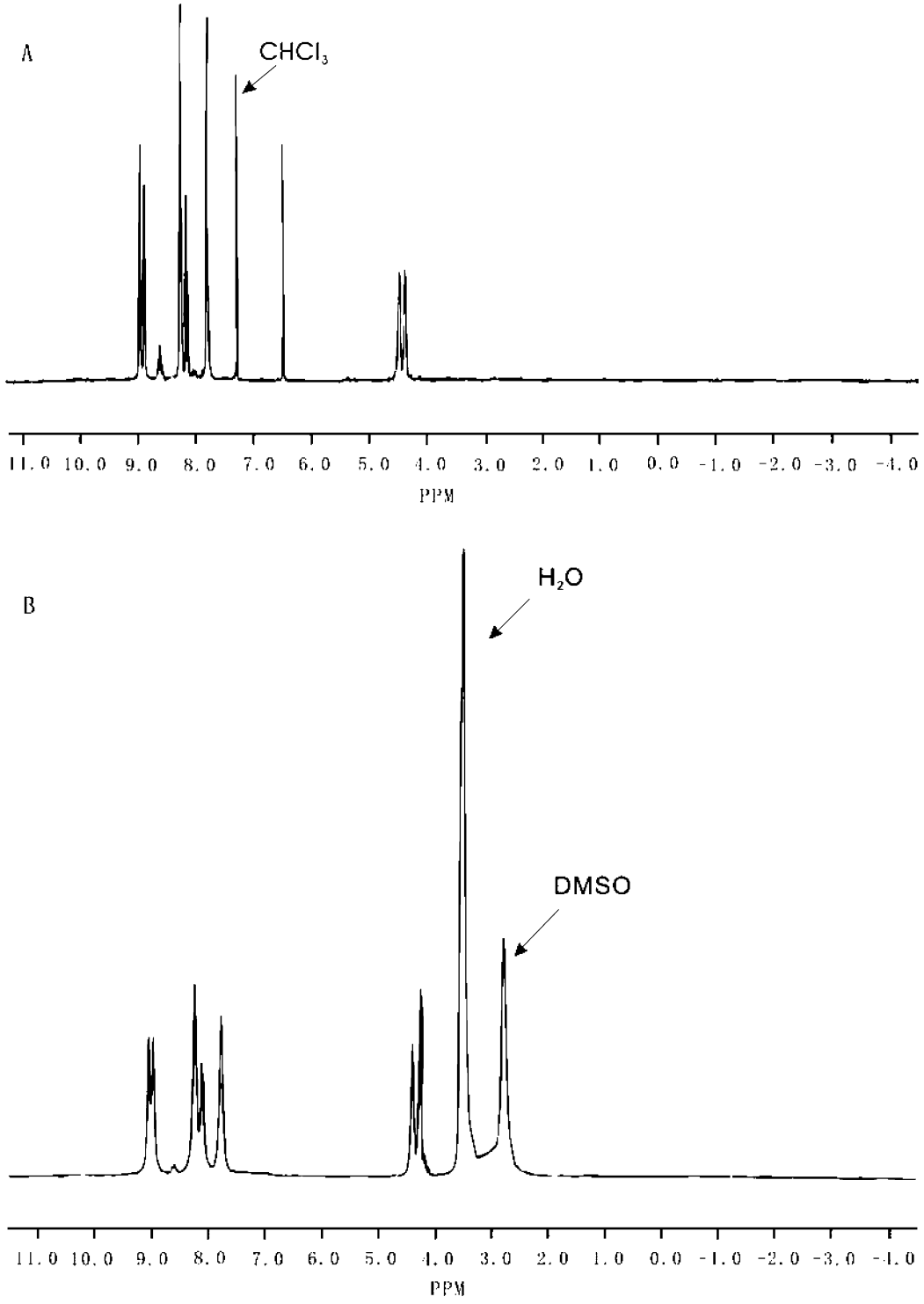

Fig. 6. ^{1}H NMR spectra of the monomer **1** (A) and the Polymer **poly1** (B).

DMSO is compared with those of the **poly1** on the ITO transparent electrode as well as the dissolved polymer in DMSO (Fig. 5). Upon the film formation, Soret band and Q bands shift to long wavelength along with peak broadening. The red shift as well as considerable broadness of the Soret band was previously observed in the case of several supported porphyrins, and were attributed to severe degree of aggregation and stacking of the porphyrin molecules on the electrode surface [33]. When the deposited polymer was dissolved in DMSO, the nearly same UV/vis spectrum as that of the corresponding monomer was produced, but with larger peak broadness.

Fig. 6 displays the ^{1}H NMR spectrum of the monomer **1** together with that of the **poly1** dissolved

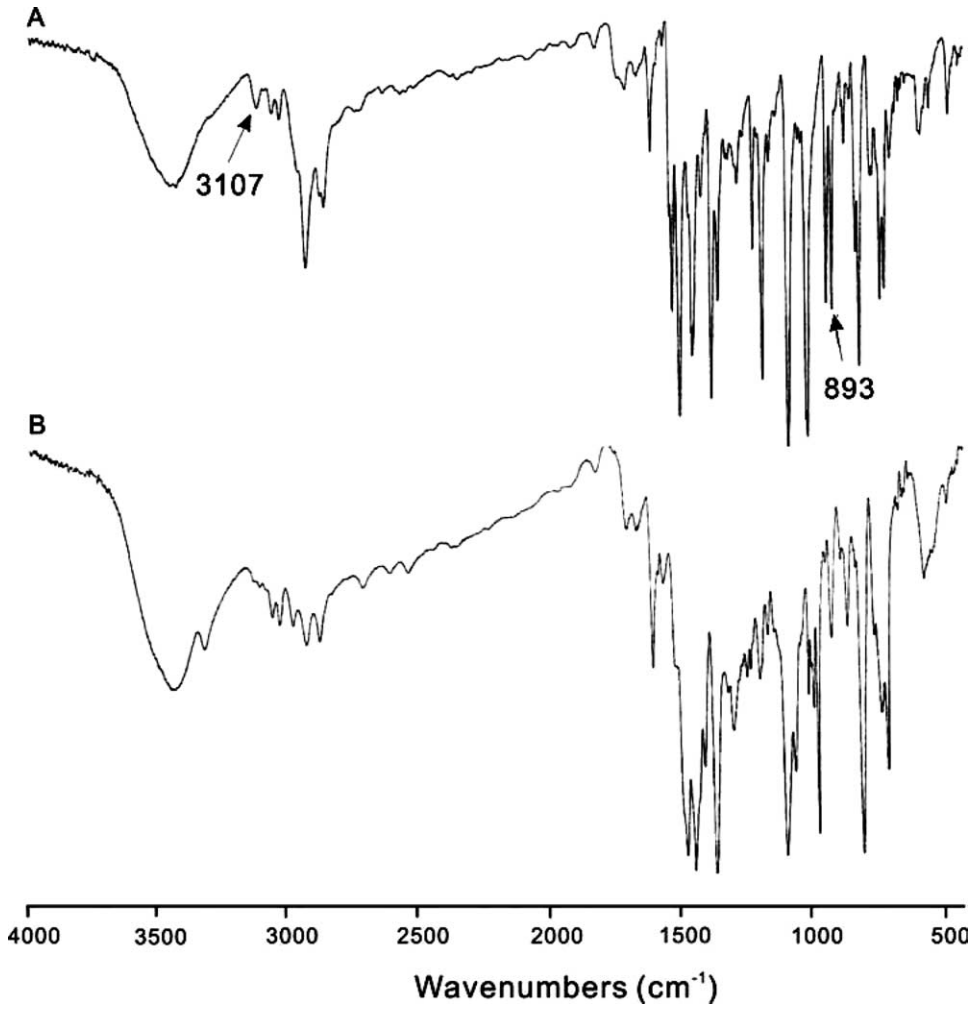

Fig. 7. FT-IR spectra of the monomer **1** (A) and the polymer **poly1** (B).

from electrode surface. Comparison of both spectra shows that, after the polymerization reaction, the singlet signal at 6.43 ppm attributable to the lone thienyl proton [42] completely disappeared, indicating the occurence of α–α' couplings of the thiophene rings and the formation of a reasonably high molecular weight polymer with no visible end groups. MALDI-TOF MS was employed to find out the polymerization degree in **poly1**. However,

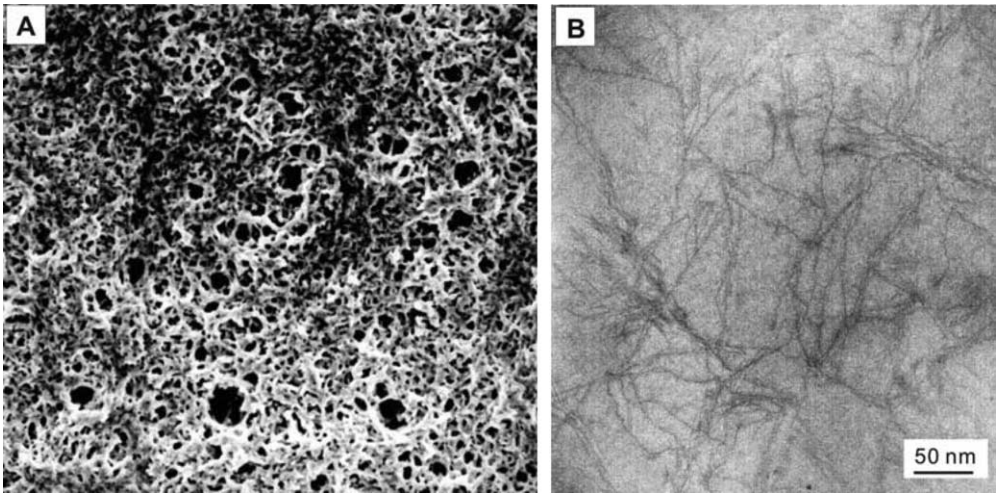

Fig. 8. SEM image of the deposited polymer on ITO (A) and TEM image of the dissolved polymer in DMSO (B).

the experiments failed, because no appropriate matrix was found.

Complementary to the ^{1}H NMR data, the analysis of the FT-IR spectra of the monomer **1** and the **poly1** also suggests α–α' couplings of the thiophene rings during polymerization. FTIR spectrum of the monomer **1** exhibited the characteristic α-CH out of plane bending at 893 cm^{-1} and α-CH stretching of the thiophene ring at 3107 cm^{-1}, respectively (Fig. 7(A)) [43,44]. After polymerization reaction these absorption peaks were absent in the spectrum of the obtained **poly1** (Fig. 7(B)). These results further indicate that the polymerization of the synthesized monomer proceeds through the α–α' couplings of the thiophene rings.

Examination by scanning electron microscopy showed that the deposited polymer films on different electrode surfaces exhibit a homogeneous morphology (Fig. 8(A)). A 10 μl aliquot of DMSO solution of polymer (**poly1**) was dropped onto a holey carbon coated copper grid. After desposition for 1 min, the remaining solution was wiped up using filter paper and polymer chains were imaged by transmission electron microscopy. Long fabric aggregate in submicrometer range was observed (Fig. 8(B)).

4. Conclusions

We report the synthesis and electropolymerization of two new thiophenesubstituted porphyrins and their zinc complexes. It is found that the porphyrin with 3,4-ethylenedioxythiophene units possesses good polymerizability and can be readily electropolymerized onto different electrode surfaces. Electrochemical characterizations show that the resultant polythiophene–metalloporphyrin hybrid materials are highly electroactive and exhibit remarkable higher electrochemical stability. Interestingly, they exhibit a charge-trapping effect. The formation of two different redox units in resultant polymer chains is believed to be responsible for the observed charge-trapping phenomenon, and the proposed mechanism was supported by using model compounds. The deposited polymer films on different electrode surfaces show a homogeneous morphology and are soluble in polar solvents such as DMSO or DMF. Besides electrochemical method, UV/vis, NMR, FTIR, TEM and SEM were employed to characterize the new porphyrin polymer.

Acknowledgements

The National Science Foundation of China (No. 20473044) and The Deutsche Forschungsgemeinschaft (SFB 448 ‘Mesoscopic System’) provided geneous financial support.

References

[1] Anderson HL. Chem Commun 1999;2323.
[2] Collman JP, Zhang X, Lee VJ, Uffelman US, Brauman JI. Science 1993;261:1404.
[3] Murray RW, editor. Molecular design of electrode surfaces. New York: Wiley Interscience; 1992.
[4] Bedioui F, Devynck J, Bied-Charreton C. Acc Chem Res 1995;28:30.
[5] Ohkita H, Ogi T, Kinoshita R, Ito S, Yamamoto M. Polymer 2002;43:3571.
[6] Collman JP, Denisevich P, Konai Y, Morrocco M, Koval C, Anson FC. J Am Chem Soc 1980;102:6027.
[7] Durand RR, Bencosme CS, Collman JP, Anson FC. J Am Chem Soc 1983;105:2710.
[8] Willman KW, Rocklin RD, Nowak R, Kuo KN, Schultz FA, Murray RW. J Am Chem Soc 1980;102:7629.
[9] Jester CP, Rocklin RD, Murray RW. J Electrochem Soc 1980;127:1979.
[10] Zak J, Yuan H, Ho K, Woo LK, Porter MD. Langmuir 1993;9:2772.
[11] Hutchison JE, Postlethwaite TA, Murray RW. Langmuir 1993;9:3277.
[12] Offord DA, Sachs SB, Ennis MS, Eberspacher TA, Griffin JH, Chidsey CED, et al. J Am Chem Soc 1998;120:4478.
[13] Clausen C, Cryko DT, Dabke RB, Dontha N, Bocian DF, Kuhr WG, et al. J Org Chem 2000;65:7363.
[14] Anson FC, Ni CL, Saveant JM. J Am Chem Soc 1985;107:3442.
[15] Marcor KA, Spiro JG. J Am Chem Soc 1983;105:5601.
[16] Bettelheim A, White BA, Raybuck SA, Murray RW. Inorg Chem 1987;26:1009.
[17] Medeiros MAC, Cosnier S, Deronzier A, Moutet JC. Inorg Chem 1996;35:2659.
[18] Kuester SN, McGuire MM, Drew SM. J Electroanal Chem 1998;452:13.
[19] Savenije TJ, Koehorst RBM, Schaafsma TJ. J Phys Chem B 1997;101:720.
[20] Schaeferling M, Baeuerle P. Synth Met 2001;119:289.
[21] Schaeferling M, Baeuerle P. Synth Met 1999;101:38.
[22] Takeuchi M, Shioya T, Swager TM. Angew Chem 2001;113:3476.
[23] Kingsborough RP, Swager TM. Angew Chem 2000;112:3019.
[24] Segawa H, Wu FP, Nakayama N, Mariyama H, Sagisaka S, Higuchi N, et al. Synth Met 1995;71:2151.
[25] Shimidzu T. Synth Met 1996;81:235.
[26] Ballarin B, Masiero S, Seeber R, Tonelli D. J Electroanal Chem 1998;449:173.
[27] Littler BJ, Miller MA, Hung CH, Wagner RW, O’Shea DF, Boyle PD, et al. J Org Chem 1999;64:1391.
[28] Mohanakrishnan AK, Hucke A, Lyon MA, Lakshmikantham MV, Cava MP. Tetrahedron 1999;55:11745.
[29] Lee CH, Lindsey JS. Tetrahedron 1994;50:11427.
[30] Deronzier A, Devaux R, Limosin D, Latour JM. J Electroanal Chem 1992;324:325.
[31] Abruna HD, Denisevich P, Umana M, Meyer TJ, Murray RW. J Am Chem Soc 1981;103:1.
[32] Denisevich P, Willman KW, Murray RW. J Am Chem Soc 1981;103:4727.
[33] Smith DK, Lane GA, Wrighton MS. J Am Chem Soc 1986;108:3522.
[34] Smith DK, Lane GA, Wrighton MS. J Phys Chem 1988;92:2616.
[35] Smith DK, Tender LM, Lane GA, Licht S, Wrighton MS. J Am Chem Soc 1989;111:1099.
[36] Hable CT, Crooks RM, Valentine JR, Giasson R, Wrighton MS. J Phys Chem 1993;97:6060.
[37] Ramachandraiah G, Bedioui F, Devynck J, Serrar M, Bied-Charreton C. J Electroanal Chem 1991;319:395.
[38] Trevin S, Bedioui F, Devynck J. J Electroanal Chem 1996;408:261.

[39] Sotzing GA, Thomas CA, Reynolds JR, Steel PJ. Macromolecules 1998;31:3752.
[40] Ahonen HJ, Lukkari J, Kankare J. Macromolecules 2000;33:6787.
[41] Krishnamoorthyk K, Ambade AV, Mishra SP, Kanungo M, Contractor AQ, Kumar A. Polymer 2002;43:6465.
[42] Kumar A, Reynolds JR. Macromolecules 1996;29:7629.
[43] Sakmeche N, Aeiyach S, Aaron JJ, Jouini M, Lacroix JC, Lacaze PC. Langmuir 1999;15:2566.
[44] Yilmaz F, Cianga L, Guner Y, Toppare L, Yagci Y. Polymer 2004;45:5765.